PLANAR LASER-INDUCED FLUORESCENCE MEASUREMENTS OF HIGH-ENTHALPY FREE JET FLOW WITH NITRIC OXIDE*

Jennifer L. Palmer, Brian K. McMillin, and Ronald K. Hanson

High Temperature Gasdynamics Laboratory

Department of Mechanical Engineering

Stanford University, Stanford, CA 94305-3032

SUMMARY

Planar laser-induced fluorescence (PLIF) measurements of property fields in a high-enthalpy, supersonic, underexpanded free jet generated in a reflection-type shock tunnel are reported. PLIF images showing velocity and temperature sensitivity are presented. The inferred radial velocity and relative rotational temperature fields are found to be in agreement with those predicted by a numerical simulation of the flowfield using the method of characteristics.

INTRODUCTION

Planar laser-induced fluorescence (PLIF) has been used in a variety of experiments to visualize gas flows and to give limited information about their aero-thermochemical properties. Recently, interest has shifted towards variations of PLIF which allow quantitative velocity and temperature measurements. The goal of the present work is to develop experimental methods for making quantitative, single-shot measurements of several properties in a high-stagnation condition supersonic flowfield using PLIF of nitric oxide (NO) [1,2], a species naturally present in many flowfields of practical importance. Extension of PLIF techniques to truly quantitative measurements will provide the capability for detailed analysis of flowfields of interest to the aeronautics and propulsion communities and will allow improved experimental validation of computational fluid dynamics models.

Several velocimetry studies have been performed previously using time- or frame-averaged PLIF imaging of NO [3,4] and molecular iodine (I_2) [5]. In the present work, single-shot PLIF images have been used to provide an instantaneous measurement of the radial velocity field in a high-stagnation temperature, high-speed free jet under the assumption that the flowfield is axisymmetric.

One- and two-line PLIF thermometry techniques have been applied in a variety of flowfields using several fluorescent species, including NO,[6-8] I_2,[5,9] molecular oxygen (O_2),[7,10] and the hydroxyl radical (OH).[7,11-13] Time- or frame-averaged images have been obtained with I_2 and NO,[5,7] while instantaneous PLIF temperature measurements have been limited to NO[6,8] or O_2 in isobaric, constant mole-fraction flows[7] or to OH in reacting flows.[11-13] Here, single-shot images obtained by exciting transitions from different rotational levels have been used in measuring the temperature field throughout the free jet.

The experiments to be discussed here were performed in a reflection-type shock tunnel facility in which a high-enthalpy, underexpanded free jet is created. The test gas was argon seeded with a small amount of NO. A schematic of a high-pressure ratio free jet is shown in figure 1 with its primary features labelled. This flowfield exhibits extreme variations in pressure and temperature, as well as high speed, which make it a challenging and appropriate environment in which to pursue the development of PLIF for more complex supersonic/hypersonic flows.

In the following sections, a brief description of the PLIF method is given and requirements for quantitative measurements in the shock tunnel free jet flow are discussed. The experimental facility and techniques are described, and PLIF images of the velocity and temperature fields are presented. The experimental results are compared with predictions made using a method of characteristics (MOC) simulation to assess their accuracy and to identify areas where improvement is needed.
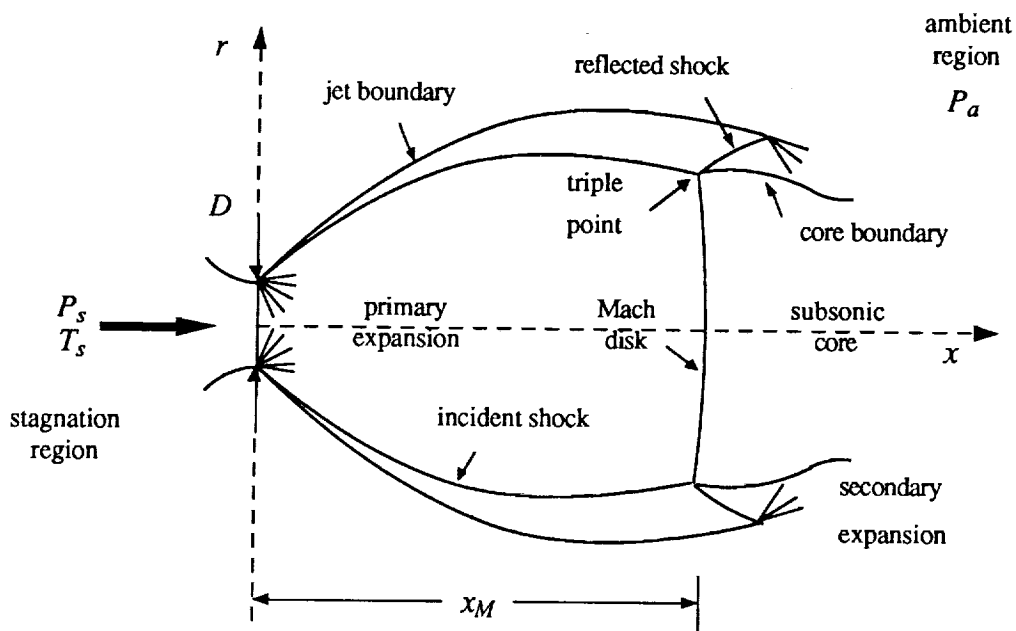

Figure 1. Schematic of underexpanded, supersonic free jet flowfield.

PLIF TECHNIQUES

PLIF experiments utilize a thin sheet of laser light, directed through the flowfield in the desired plane of observation. The laser is tuned to resonantly excite a particular electronic transition of a molecular species present in the flow; pulsed lasers are used to provide an essentially instantaneous view of the flowfield. A portion of the fluorescent radiation is collected perpendicular to the observation plane by an optical system and imaged onto a two-dimensional solid-state array. The resultant temporally integrated signal is then analyzed to extract a spatially resolved property field. In this experiment, excitation of several electronic transitions in the $A^2\Sigma^+\leftarrow X^2\Pi(0,0)$ band of NO at ~226 nm is used with broadband fluorescence detection.

The total fluorescence signal for weak excitation of an isolated absorption line is given by:

$$S_f = E_p\, g\, B\, N_a f_{v''J''}(T) \left(\frac{A}{A+Q}\right) C_{opt}, \tag{1}$$

where E_p is the laser pulse energy; g is the spectral convolution of the laser and absorption lineshapes; A and B are Einstein coefficients; N_a is the mole fraction of the absorbing species; T is the temperature; $f_{v''J''}(T)$ is the Boltzmann fraction of the absorbing state; Q is the electronic quenching rate of the excited state; C_{opt} is a constant dependent upon the optical arrangement, collection efficiency, etc.

S_f is also sensitive to the Doppler shift of the absorption induced by the bulk motion of the flow in the direction of laser propagation. In the experimental arrangement used here, laser light propagates perpendicularly through the jet axis. The Doppler shift is thus proportional to the radial component of the velocity, V_r. Since the flowfield is symmetric, the signals $S_f(x,r)$ and $S_f(x,-r)$ result from identical thermodynamic conditions and equal-but-opposite Doppler shifts. For a Gaussian laser lineshape significantly broader than the absorption line, the following expression may be used to obtain V_r from the fluorescence signal:[1]

$$\frac{S_f(x,r) - S_f(x,-r)}{S_f(x,r) + S_f(x,-r)} = \tanh\left\{8\ln 2\; \nu_a \frac{V_r}{c} \frac{\nu_a - \nu_l}{\Delta\nu_l^2}\right\}, \tag{2}$$

where ν_a and ν_l are the center frequencies of the absorption and laser lines, respectively; $\Delta\nu_l$ is the FWHM of the laser lineshape; and c is the speed of light. The right-hand-side of this equation may be simplified for small values of the argument, yielding a linear relationship between the processed signal and the radial velocity. Use of the linearized form can be the source of substantial systematic error in velocity measurements.[3]

Another excitation and processing technique is used to measure the rotational temperature field.[8] A ratio of signals $S_{f1}(x,r)$ and $S_{f2}(x,r)$ obtained with the laser tuned first to excite one transition and then another from a different rotational state, but the same lower vibrational level gives the result:

$$R(x,r,T) = \frac{S_{f1}(x,r)}{S_{f2}(x,r)} = C_{12} \exp\left\{- \frac{\left[F(J''_1)-F(J''_2)\right]}{kT}\right\}. \tag{3}$$

Here C_{12} is a constant dependent on the ratio of the laser energies, spectral convolutions, Hönl-London factors (the rotationally-dependent part of B), lower state population degeneracies, collection efficiencies, etc. To avoid amplification of existing random error in the inferred temperature, $F(J''_1)-F(J''_2) \geq kT$ is required. Note that throughout the temperature measurements to be discussed here, the laser was tuned to line center and passed perpendicularly through the jet axis. The images are thus symmetric, i.e., $S_f(x,r) = S_f(x,-r)$.

Because a single excitation/collection system is used at present, temperature-sensitive images with different J'' must be acquired individually. Reproducibility when combining temperature-sensitive images and a symmetric flowfield for velocity extraction from a single image are required. Fortunately, the inviscid core of the free jet flowfield is extremely symmetric and repeatable, except for some slight shot-to-shot variation in the shock position. Instantaneous velocity and temperature fields in the turbulent portions of the flowfield, such as in the shear layer where jet fluid meets the ambient, are not captured with this method, however.

EXPERIMENTAL FACILITY

Shock Tunnel System

The facility in which these experiments were performed may be operated either as a shock tube or as a shock tunnel. The performance characteristics of the shock tube are well known, as it has been used previously in several gasdynamic studies.[8] Shock tunnel characterization has also been carried out.[1,2] Figure 2 shows a schematic of the facility, along with the optical and electronic components required for PLIF imaging of the flowfield.

A large range of stagnation conditions, P_s and T_s, are available for experiments in the shock tunnel with an initial loading of Ar (or 2% NO in Ar) at room temperature.[2] In all of the experiments, a test gas mixture of 2% NO in Ar initially at 20 torr was loaded into the shock tube, which yielded an incident shock with average Mach number $M_s = 4.20 \pm 0.05$. Calculations[14]
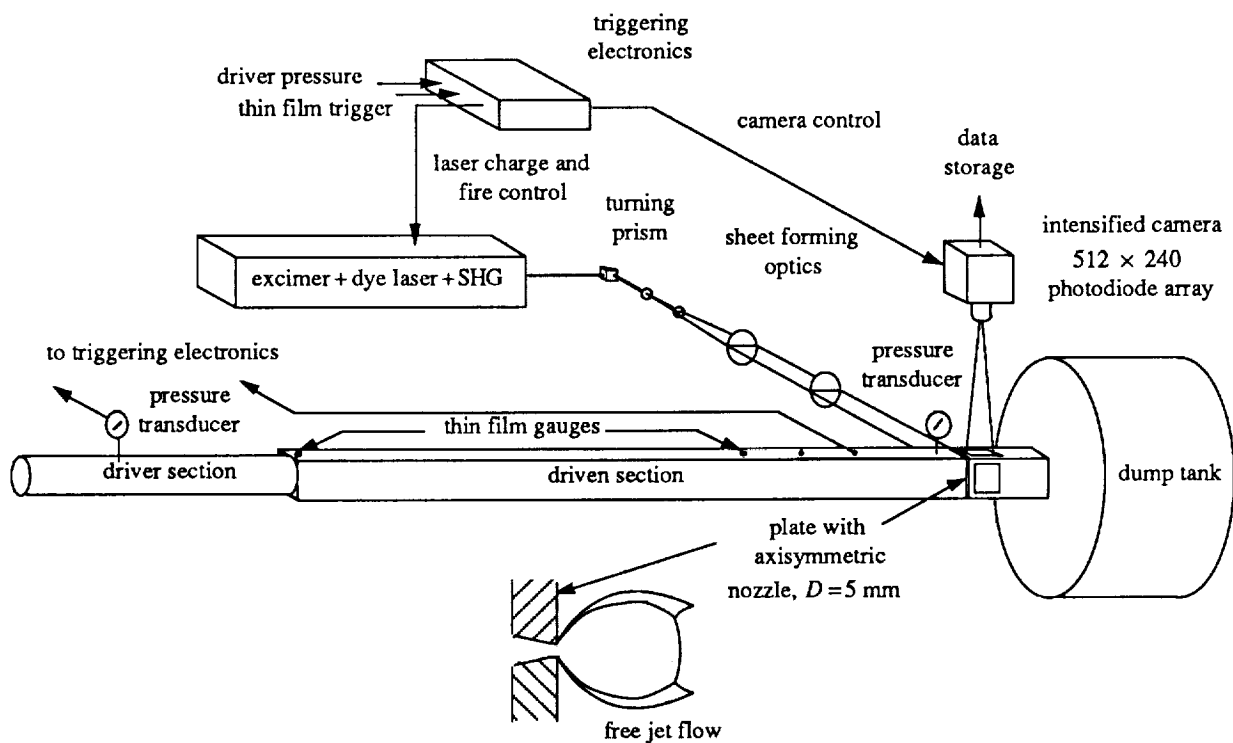
Figure 2. Schematic of experimental facility with associated optical and electronic components for PLIF imaging.

based on the actual shock tube performance indicate that the reservoir conditions were $T_s = 4200 \pm 200$ K and $P_s = 3.00 \pm 0.10$ atm. Since the ambient region of the flowfield was decoupled from the initial loading of the shock tube by the presence of a diaphragm at the nozzle, P_s/P_a may be adjusted independently for a given set of stagnation conditions. Pure Ar at 10 torr formed the ambient of the free jet flowfield, yielding $P_s/P_a \approx 230$. PLIF images were acquired shortly after the jet became fully developed.

PLIF Imaging System

Frequency-doubled light from a broadband, tunable XeCl-pumped dye laser with Coumarin 450 dye was used to excite several transitions in the $A^2\Sigma^+ \leftarrow X^2\Pi(0,0)$ band of NO. The frequency-doubled output of the laser was ~0.5 mJ/pulse with a spot size ~2 mm in diameter. A combination of cylindrical lenses was used to form a thin, collimated sheet of laser light. The sheet propagated through the axis of the free jet, where it was ~5 cm wide and ~0.4 mm thick. The laser detuning (~0.13 cm^{-1}) and Gaussian linewidth (~0.36 cm^{-1}) were measured just prior to each velocity experiment with an etalon for use in equation 2.
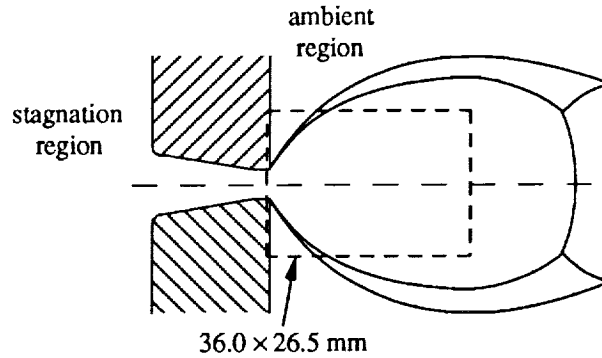
Figure 3. Imaging geometry for PLIF experiments.

An electronic delay sequence initiated firing of the laser/intensifier/camera system to allow observation of the jet flowfield at the proper time during the shock tunnel transient. The broadband fluorescence resulting from excitation of the test gas by a single laser pulse was collected normal to the direction of laser propagation, as shown in figure 2. A Cassegrainian reflecting lens imaged the fluorescence onto a single microchannel plate-intensified CCD array sampled to 512×240. The region of the flowfield imaged in the PLIF experiments is shown in figure 3. A 2 mm thick UG-5 Schott glass filter was used to block elastically scattered light. PLIF data images were corrected for background and laser sheet variations on a pixel-by-pixel basis.

RESULTS AND DISCUSSION

Velocity Imaging

The single-shot and 5-frame average radial velocity images shown in figure 4 were obtained by exciting the overlapping transitions $P_1(5)$ and $P_1(12)$ of NO. The predicted radial velocity field from the MOC calculation is shown for comparison. The signal level displayed is proportional to V_r as indicated by the grey-scale bar.

The measured velocity profiles at $x/D = 1$, 2, and 3 obtained from the image shown in figure 4(b) are shown in figure 5, along with those from the MOC. The effect of using the nonlinear velocity algorithm (equation 2), rather than its simplified, linear version is illustrated by the departure of the two inferred profiles at high values of V_r. The linear calculation systematically under-predicts V_r; although the noise in the data is amplified by the nonlinear velocity conversion algorithm. In this case, the error resulting from the use of the linear conversion algorithm is as much as 30%. For moderate V_r (up to ~1 km/s) the measured profiles follow the MOC predictions.
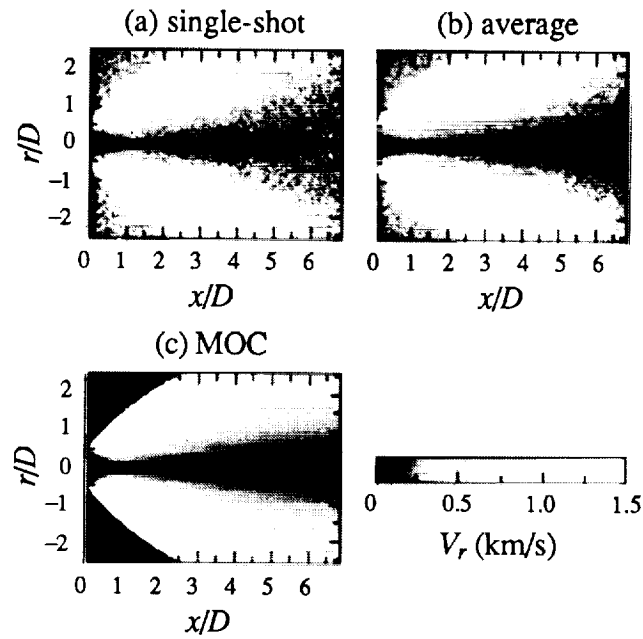
Figure 4. Radial velocity images: (a) single-shot, (b) 5-frame average, and (c) simulated by the MOC. The jet stagnation conditions were: $P_a = 3.00$ atm, $T_a = 4200$ K, $P_s/P_a = 230$ in a test gas of 2% NO in Ar.

Random error in the single-shot velocity data is a consequence of the relatively small NO concentration in the test gas and the limited dynamic range of the data collected. The unprocessed PLIF images had signal-to-noise ratios of 10:1 for small x/D ($\leq$ 2), with minimum levels of ~5:1 at large x/D ($\geq$ 5). Random fluctuations of ± 50-100 m/s occur in the velocity data obtained from an average image at small x/D, as shown in figure 5.
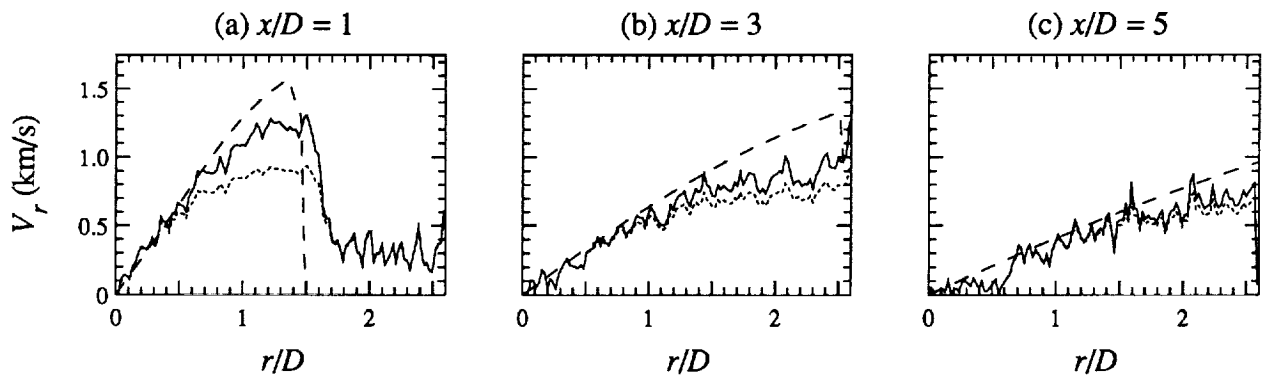

Figure 5. Average measured and calculated radial velocity distributions as a function of normalized radial distance from the jet axis at several axial locations at (a) $x/D = 1$, (b) $x/D = 3$, and (c) $x/D = 5$. The velocity inferred with the nonlinear algorithm is shown with a solid line and the linear result with a dotted one. MOC results are shown with a dashed line.

The systematic error present mainly at large V_r probably results from laser lineshape uncertainties and from the insensitivity of the measurement to velocity when $\Delta v_D \gtrsim v_a - v_l$, as well.[3] Saturation of the absorption is another source of error which would result in an inferred V_r lower than expected, particularly at large x/D, where saturation is most likely to occur.

Temperature Imaging

Four ro-vibronic transitions from different J'' states were used in measuring the rotational temperature field of the free jet. The limited dynamic range of the data, coupled with the requirement for $F(J''_1) - F(J''_2) \geq kT$ necessitates the use of more than two transitions to obtain a temperature field with acceptable signal-to-noise throughout. The raw single-shot images exhibit signal-to-noise of 10:1 or better. Images obtained from ratios of individual single-shots as well as from 5-frame average images for two of the six possible line pair combinations are displayed in figure 6. Simulated temperature-dependent fields are shown for comparison. The relative logarithmic conversion from $R(x,r,T)$ to T is illustrated by the grey-scale bar labels for each set.
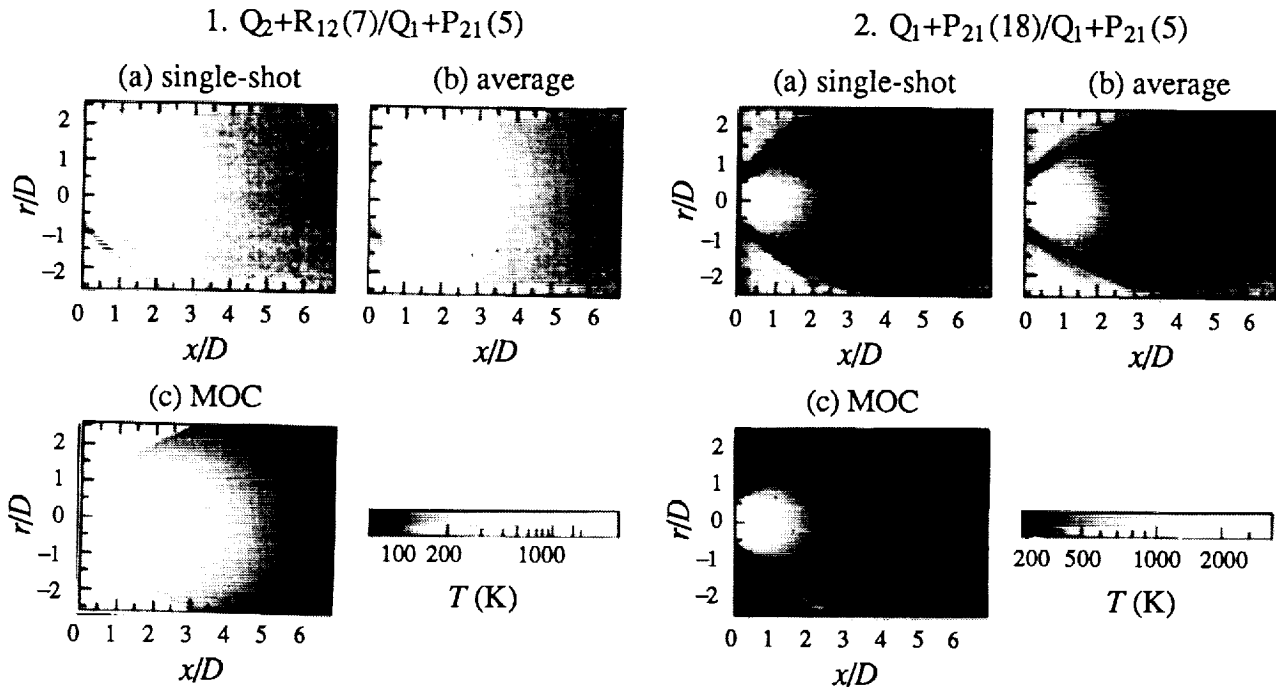

Figure 6. Temperature images: (a) single-shot, (b) 5-frame average, and (c) simulated using the MOC for two line pair ratios: 1. $Q_2 + R_{12}(7)/Q_1 + P_{21}(5)$ and 2. $Q_1 + P_{21}(18)/Q_1 + P_{21}(5)$. The jet stagnation conditions were: $P_a = 3.00$ atm, $T_a = 4200$ K, $P_s/P_a = 230$ in a test gas of 2% NO in Ar.

The images of figures 6.1(a) and (b) for the line pair ratio $Q_2+R_{12}(7)/Q_1+P_{21}(5)$ show a slowly decreasing signal ratio with increasing x/D, as would be expected with falling temperature. The increasing signal in the PLIF images for $Q_1+P_{21}(18)/Q_1+P_{21}(5)$ at large x/D resulted from noise present in that portion of the individual images making up the ratio, exacerbated by the limited dynamic range of the data. For this reason, only the temperature measured in the region $x/D \lesssim 5$ is valid using the line pair combination $Q_1+P_{21}(18)/Q_1+P_{21}(5)$. Also, very near the nozzle exit, the temperature inferred from any of the line pair combinations may be flawed due to emission and/or to the larger absorption linewidth there. Each line pair ratio has for similar reasons, a limited range of validity.

Figure 7 shows the temperature variation along the jet axis inferred from several line pair combinations. The data for each ratio was obtained using average images for the individual line pairs and is displayed only within the limits discussed above. The axial temperature distribution from the MOC simulation is found to be very well reproduced by the data for $0.2 \le x/D \le 6.8$. The radial temperature distribution at any given axial location has also been found to be accurately measured using a combination of several line pairs. A uniformly valid average rotational temperature field was obtained with a signal-to-noise ratio of $\ge 20{:}1$ throughout the region $0.2 \le x/D \le 6.8$ from single-shot raw data images with signal-to-noise of $10{:}1$ or better.
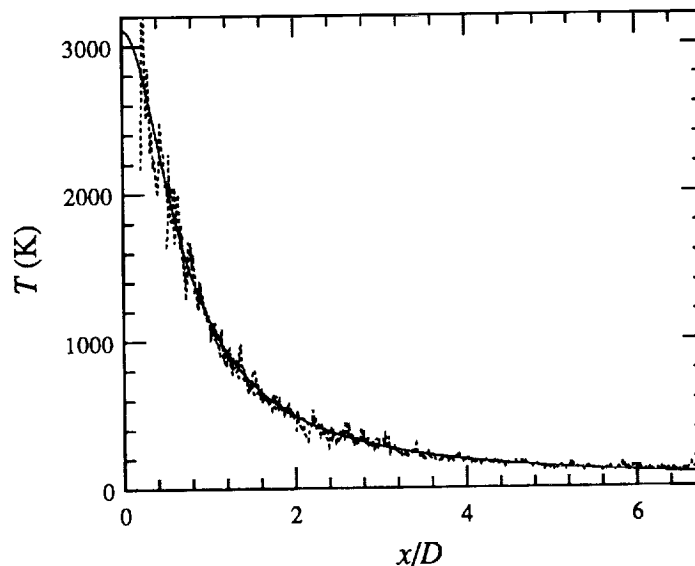

Figure 7. Relative measured and calculated rotational temperature as a function of distance along the jet axis. The temperatures inferred from several average PLIF image ratios are shown with dotted lines. The results shown are from line pair ratios: $Q_1+P_{21}(28)/Q_2+R_{12}(7)$ $(0.2 \le x/D \le 2.0)$, $Q_1+P_{21}(28)/Q_1+P_{21}(5)$ $(0.5 \le x/D \le 2.0)$, $Q_1+P_{21}(18)/Q_1+P_{21}(5)$ $(1.0 \le x/D \le 3.0)$, and $Q_2+R_{12}(7)/Q_1+P_{21}(5)$ $(2.0 \le x/D \le 6.8)$. MOC results are shown with a solid line.

CONCLUSIONS

PLIF imaging of NO has been used in the measurement of velocity and temperature fields in a supersonic, high-stagnation condition, free jet flowfield. Experimental techniques for obtaining quantitative measures of the radial velocity and the rotational temperature were discussed. Application of these methods yielded velocity and temperature fields in good agreement with predictions made using the MOC.

The radial component of velocity was obtained from single-shot PLIF images to give an instantaneous field in the core of the jet. Accurate values of the laser parameters upon which the spectral convolution and, hence, the processed signal depend were used in converting the PLIF signal to velocity. The full, nonlinear form of the velocity conversion algorithm was used in processing the data; and the results compared well with those from the MOC calculation of the flowfield, up to ~1 km/s. Substantial deviation from the nonlinear result was found to occur from use of the linear velocity conversion in regions of the jet with large velocities. Single-shot and average radial velocity images were found to have random fluctuations of ±100-200 m/s and ±50-100 m/s, respectively, having been calculated from PLIF images with maximum signal-to-noise ratios of 10:1 and 20:1.

The strategy implemented for temperature imaging involved the use of several different transitions to obtain a valid measurement with acceptable random fluctuations throughout the free jet flowfield. Single-shot images for each of the four line pairs used had signal-to-noise ratios greater than 10:1. Correspondingly, average images showed random fluctuations of less than ±5%. Different line pair combinations were found to be of use in calculating the temperature field in different portions of the jet. The range of validity for each ratio of average images was limited to the overlap of the areas in the raw images where adequate signal above background was recorded. Another limit on the use of a given line pair combination arose from the undesirable amplification of noise in areas with large temperature relative to the energy spacing of the two line pairs.

The conversion from signal ratio to temperature was performed in each case by normalizing the measured ratio along a portion of the jet axis to that predicted by the MOC. Generally, excellent agreement was found between the measured and calculated temperature fields in the inviscid core of the jet for $0.2 \leq x/D \leq 6.8$. The temperature field resulting from an amalgamation of several line pair ratios typically showed random fluctuations of ±5%. Maximum random error of ±10-15% was observed close to the nozzle exit, where the temperature was significantly higher than the equivalent energy spacing for the line pair combination used.

The shock tunnel facility has proven useful as a ground test facility, as it provides dependable high-enthalpy supersonic flow conditions at low cost. Successful measurement of some of the flowfield parameters of interest has been carried out using PLIF of NO and reported here. In the future, development of quantitative PLIF techniques will continue, with extension planned to axial velocity and vibrational temperature field measurements, for example.

ACKNOWLEDGEMENT

REFERENCES

1. J.L. Palmer, B.K. McMillin, and R.K. Hanson, "Planar-Laser Induced Fluorescence Imaging of Underexpanded Free Jet Flow in a Shock Tunnel Facility," AIAA-91-1687, Jun., 1991.

2. J.L. Palmer, B.K. McMillin, and R.K. Hanson, "Planar-Laser Induced Fluorescence Imaging of Velocity and Temperature in Shock Tunnel Free Jet Flow," AIAA-92-0762, Jan., 1992.

3. P.H. Paul, J.M. Seitzman, M.P. Lee, J.L. Palmer, and R.K. Hanson, "Planar Laser-Induced Fluorescence Imaging in Supersonic Flows," AIAA-89-2912, Jul., 1989.

4. P.H. Paul, M.P. Lee, R.K. Hanson, "Molecular Velocimetry Imaging of Supersonic Flows Using Planar Laser-Induced Fluorescence of NO," *Optics Letters*, Vol. 14, 1989, pp. 417-421.

5. R.J. Hartfield, Jr., S.D. Hollo, and J.C. McDaniel, "A Unified Planar Measurement Technique for Compressible Flows Using Laser-Induced Iodine Fluorescence," AIAA-92-0141, Jan., 1992.

6. J.M. Seitzman, G. Kychakoff, and R.K. Hanson, "Instantaneous Temperature Field Measurements Using Planar-Laser Induced Fluorescence," *Optics Letters*, Vol. 10, 1985, pp. 439-441.

7. R.K. Hanson, J.M. Seitzman, and P.H. Paul, "Planar Laser-Induced Fluorescence Imaging of Combustion Gases," *Applied Physics B*, Vol. 50, 1989, pp. 441-454.

8. B.K. McMillin, J.L. Palmer, and R.K. Hanson, "Two-Dimensional Temperature Measurements of Nonequilibrium Supersonic Flows Using Planar Laser-Induced Fluorescence of Nitric Oxide," AIAA-91-1670, Jun., 1991.

9. T. Ni-Imi, T. Fujimoto, and N. Shimizu, "Method for Planar Measurement of Temperature in Compressible Flow Using Two-Line Laser-Induced Iodine Fluorescence," *Optics Letters*, Vol. 15, 1990, pp. 918-920.

10. M.P. Lee, P.H. Paul, and R.K. Hanson, "Quantitative Imaging of Temperature Fields in Air Using Planar Laser-Induced Fluorescence of O_2," *Optics Letters*, Vol. 12, 1987, pp. 75-77.

11. P.H. Paul and R.K. Hanson,"Applications of Planar Laser-Induced Fluorescence Imaging Diagnostics to Reacting Flows," AIAA-90-1844, Jul., 1990.

12. M.G. Allen, S.J. Davis, and K. Donohue, "Planar Measurements of Instantaneous Species and Temperature Distributions in Reacting Flows: A Novel Approach to Ground Testing Instrumentation," AIAA-90-2383, Jul., 1990.

13. P.H. Paul, U.E. Meier, and R.K. Hanson, "Single-Shot, Multiple-Camera Planar Laser-Induced Fluorescence Imaging in Gaseous Flows," AIAA-91-0459, Jan., 1991.

14. A.G. Gaydon and I.R. Hurle, *The Shock Tube in High-Temperature Chemical Physics*, Reinhold, NY, 1963.